Send Orders for Reprints to reprints@benthamscience.ae

Current Pharmaceutical Design, 2017, *23*, 1-8

RESEARCH ARTICLE

Biotin and Glutathione Targeting of Solid Nanoparticles to Cross Human Brain Endothelial Cells

Szilvia Veszelka[a], Mária Mészáros[a], Lóránd Kiss[a,#], Zoltán Kóta[a], Tibor Páli[a], Zsófia Hoyk[a], Zsolt Bozsó[b], Lívia Fülöp[b], András Tóth[a,c], Gábor Rákhely[a,c] and Mária A. Deli[a,*]

[a]*Institute of Biophysics, Biological Research Centre of the Hungarian Academy of Sciences, Temesvári krt. 62, H-6726 Szeged, Hungary;* [b]*Department of Medical Chemistry, University of Szeged, Dóm tér 8, H-6720 Szeged, Hungary;* [c]*Department of Biotechnology, Faculty of Science and Informatics, University of Szeged, Középfasor 52, H-6726 Szeged, Hungary*

ARTICLE HISTORY

Received: March 31, 2016
Accepted: July 12, 2016

DOI:
10.2174/1381612823666170727144450

Abstract: ***Background*:** The blood-brain barrier restricts drug penetration to the central nervous system. Targeted nanocarriers are new potential tools to increase the brain entry of drugs. Ligands of endogenous transporters of the blood-brain barrier can be used as targeting vectors for brain delivery of nanoparticles.

***Objective*:** We tested biotin-labeled solid nanoparticles for the first time and compared to biotinylated glutathione-labeled nanoparticles in brain endothelial cells.

***Method*:** Neutravidin coated fluorescent polystyrene nanoparticles were derivatized with biotin and biotinylated glutathione. As a human *in vitro* blood-brain barrier model hCMEC/D3 brain endothelial cells were used. Cell viability by MTT test, uptake and transfer of the nanoparticles across the endothelial monolayers were measured. The uptake of the nanoparticles was visualized by confocal microscopy.

***Results*:** The tested nanoparticles caused no change in cell viability. The uptake of biotin- and glutathione-labeled nanoparticles by brain endothelial cells was time-dependent and significantly higher compared to non-labeled nanoparticles. The penetration of the glutathione-labeled nanoparticles across the endothelial monolayer was higher than the biotin-targeted ones. Biotin- and glutathione-targeted nanoparticles were visualized in hCMEC/D3 cells. We verified that hCMEC/D3 express mRNA for sodium-dependent multivitamin transporter (SMVT/SLC5A6) responsible for the blood-brain barrier transport of biotin.

***Conclusion*:** Biotin as a ligand increased the uptake and the transfer of nanoparticles across brain endothelial cells. Biotinylated glutathione could further increase nanoparticle permeability through endothelial monolayers supporting its use as a brain targeting vector.

Keywords: Biotin, blood-brain barrier, brain endothelial cell, glutathione, solute carriers, solid nanocarriers, targeted nanoparticle.

1. INTRODUCTION

Pharmaceutical treatment of most disorders of the central nervous system (CNS), like neurodegenerative diseases, stroke or brain tumors, is far from satisfactory due to the poor penetration of therapeutic drugs to the brain [1]. The blood-brain barrier (BBB) is a major obstacle to prevent potential neuropharmaceuticals, especially new biopharmacons, nucleic acids, peptide or protein drugs, to reach their targets in the CNS [2]. The barrier is formed by brain endothelial cells lining the cerebral capillaries, and plays an important role in the homeostatic regulation of the brain microenvironment necessary for the stable and co-ordinated activity of neurons [3]. The major mechanisms at the level of the BBB to limit drug transport are the complex intercellular tight junctions (TJs) between brain endothelial cells restricting the paracellular permeability, the low level of non-specific vesicular transendothelial transport, and efflux transporters which deliver metabolites from brain to blood and prevent the entry of xenobiotics and drugs to the CNS [3, 4]. The restricted paracellular and transendothelial transport pathways result in the low CNS entry of hydrophilic drugs, while the active efflux transporters of brain endothelial cells limit the brain penetration of lipophilic drugs. There is a huge research effort to develop drug delivery systems for the CNS.

*Address correspondence to this author at the Institute of Biophysics, Biological Research Centre of the Hungarian Academy of Sciences, Temesvári krt. 62, H-6726 Szeged, Hungary; Tel: +36 62 599 602; Fax: +36 62 433 133; E-mail: deli.maria@brc.mta.hu

Present address: [#]Department of Pathophysiology, University of Szeged, Semmelweis u. 1, H-6701 Szeged, Hungary

In the last two decades the potential of nanoparticles (NPs) as drug carriers including vesicular and solid NPs is increasingly investigated for drug delivery across the BBB [5, 6]. The most successful approaches target specifically the endogenous transport systems at the BBB. While the receptor-mediated transport systems of brain endothelial cells have been investigated as a way of drug delivery across the BBB for several decades [2] other physiological pathways, especially the carrier systems of the BBB have been studied only recently for CNS delivery [7]. Carrier-mediated transport at the BBB is saturable, bi-directional and supplies the CNS with nutrients such as hexoses, amino acids, monocarboxylic acids, vitamins, nucleosides, purine and pyrimidine bases, fatty acids, ions, organic anions and organic cations [8]. About 40 members of the solute carrier (SLC) family were identified in brain microvessels by serial analysis of gene expression [9]. SLCs have been neglected in biomedical research despite their huge number and their potential as drug and drug delivery targets [10].

In contrast to NPs targeted by antibodies or peptides for CNS delivery, there are only few papers describing NPs labeled with ligands of nutrient transporters present at the BBB. Gold NPs covalently labeled with glucose, a ligand of hexose transporters was transferred better than unlabeled NPs across hCMEC/D3 human brain endothelial cell monolayers [11], a human *in vitro* BBB model [12, 13]. Although the paracellular tightness of hCMEC/D3 cell line does not make it a suitable BBB model for small drug screening [13], it is widely used to study the penetration of NPs, which is a transcellular process [12]. Glucose analog-targeted vesicular NPs were used successfully to deliver vasoactive intestinal

1381-6128/17 $58.00+.00

peptide to brain in mice [14]. Phenylalanine, a ligand of the large amino acid transporter-1 (LAT-1, SLC7A5), used as a vector to target solid lipid NPs increased the transfer of the anti-HIV agent efavirenz across a BBB model *in vitro* and the drug's penetration to the brain of rats [15]. A delivery system based on dendrigraft containing doxorubicin and targeted by a choline-derivate with high affinity to choline transporter (SLC44A1) was more cytotoxic to glioma cells both *in vitro* and *in vivo* than non-targeted NPs or doxorubicin alone [16].

Glutathione (GSH) is a promising new ligand of an endogenous BBB transporter for CNS drug delivery. This tripeptide with antioxidant properties has a central role in the detoxification of intracellular metabolites. GSH is actively transported across the BBB [17], but the molecular mechanism(s) and the BBB transporter(s) are not known. Based on these original observations Gaillard *et al.* developed a BBB delivery platform [18, 19]. Pegylated liposomes targeted with GSH enhance the delivery of doxorubicin cargo across hCMEC/D3 brain endothelial cells and to brain tumors in mice [20]. Further studies confirmed the improved CNS delivery by glutathione targeted NPs of doxorubicin [21] and the opioid peptide DAMGO [22] in animal models. GSH is the only BBB targeting ligand, that is part of a brain delivery platform successfully completing phase I/IIa clinical trial [18].

Biotin (vitamin B7) is a ligand of the Na^+-dependent multivitamin transporter (SMVT/SLC5A6) which is responsible for the CNS transport of this water soluble vitamin across the BBB [8, 23]. Biotin has long been used for ligation techniques, imaging and diagnostics because of the strong interaction between biotin and avidin. Biotin-avidin technology has a potential to be applied for targeted drug therapy of tumors [24]. However, until now biotin was not tested as a potential targeting ligand of NPs to cross brain endothelial cells.

The aim of our study was to investigate biotin as a targeting ligand for solid fluorescent NPs as a simplified test system in hCMEC/D3 brain endothelial cells, an *in vitro* BBB model. We compared the efficacy of biotin targeting to glutathione-labeled NPs as a reference ligand for CNS drug delivery via targeting endogenous BBB transporter(s). In the present work unlabeled, biotin- and GSH-targeted NPs were prepared and characterized, and tested for cell viability, uptake and permeability in cultured brain endothelial cells.

2. MATERIALS AND METHODS

2.1. Materials

All reagents were purchased from Sigma-Aldrich Kft. Hungary (part of Merck Life Science), except for those specifically mentioned.

2.2. Methods

2.2.1. Synthesis of Biotinyl-6-aminohexanoyl-lysyl-glutathione

The *N*-terminal amino group of glutathione is positively charged at physiological pH. Acylation of this amino group with biotin would diminish this positive charge. To avoid the change of the overall charge of the molecule a lysine residue was built into the peptide. A 6-aminohexanoic acid spacer was also incorporated between the lysyl-glutathione and the biotin. Biotinyl-6-Ahx-Lys-γGlu-Cys-Gly-OH peptide was synthesized on Fmoc-Gly-Wang resin in 0.25 mmolar scale. Fmoc group was removed by treating the resin with 20% piperidine in DMF first for 5 min then with a new portion of the above mentioned solution for 20 min. All Fmoc protected amino acids and biotin were coupled as follows: 1 mmole of the amino acid was activated with DCC/HOBt (1 mmole each) in DMF/DCM (1:1, v/v). The coupling time was 2 hours. The reaction was monitored with qualitative ninhydrin test. If the test was positive, the coupling was repeated using HATU/DIEA activation of the amino acid. The peptide was cleaved from the resin by treating the peptide-resin with a mixture containing TFA (90 v/v%), TIS (2 v/v%), DTT (4 m/v%) and water (4 v/v%) for 15 min at 0 ºC and for 1 hour 45 min at room temperature. The peptide was then precipitated with cold diethyl ether, filtered, washed with diethyl ether, dissolved and lyophilized. The product was analyzed and purified by HPLC. Analytical analysis was done on a Hewlett-Packard Agilent 1100 Series HPLC apparatus using a Luna C18 column (100 Å, 5 µm, 250×4.60 mm, Phenomenex). Preparative chromatography was done on a Shimadzu HPLC apparatus equipped with a Luna C18 column (100 Å, 15 µm, 250×21.2 mm, Phenomenex). As eluent A and eluent B 0.1 % TFA in d.d. water (Solvent A) and 80% ACN, 0.1% TFA in distilled water (Solvent B) was used, respectively.

2.2.2. Derivatization and Characterization of Nanoparticles

Neutravidin labeled 40 nm polystyrene red fluorescent nanoparticles (TransFluoSpheres Fluorescent Microspheres, T8860, Thermo Fisher Scientific Inc., Waltham, MA USA) were used for the study. The nanoparticle suspension contained 1% solid of 7.8 nmoles/mg bearing 8.23 mmole neutravidin functionality, the density of polystyrene was 1.055 g/cm^3 in buffer (50 mM sodium phosphate, 50 mM NaCl, pH 7.5, 0.02% Tween 20, 5 mM azide). To label the nanoparticles 100 µL of suspension was incubated with 30 µL distilled water containing 3 fold molar excess of biotinyl-6-aminohexanoyl-lysyl-glutathione or biotin for 2 hours at room temperature. The different groups of nanoparticles were prepared from different batches of TransFluoSpheres. The control, non-labeled solid nanoparticles (SNP) and the derivatized biotin-labeled (SNP-B) and biotinylated glutathione-labeled (SNP-B-GSH) nanoparticles were stored at 4 ºC until the experiments (Fig. **1**). The nanoparticles were characterized for particle size and zeta potential using dynamic light scattering (Malvern Zetasizer Nano ZS, Worcestershire, UK). Before measurements, the SNPs were diluted and the final concentrations were 0.15 mg/mL in phosphate buffered saline (PBS). The mean particle size and mean zeta potential values were calculated from three measurements per sample.

2.2.3. Scanning Electron Microscopy

The morphology of nanoparticles was visualized by scanning electron microscopy (SEM; JEOL, JSM-7100F-LV, Akishima, Tokyo, Japan). Before SEM observation, a droplet of nanoparticles was diluted to 10^5 and 1 µL of the solution was pipeted onto a clean mica surface and then air-dried. After sputtering 8 nm gold on the sample, the nanoparticles were imaged in high vacuum mode at 5 kV.

2.2.4. Cell Culture

The human brain microvascular endothelial cell line hCMEC/D3 [12] was grown in MCDB 131 medium (Pan Biotech) supplemented with FBS (5%), GlutaMAX (100×, Life Technologies, USA), Chemically Defined Lipid Concentrate (100×, Life Technologies, USA), ascorbic acid (10 µg/mL), hydrocortisone (550 nM), heparin (100 µg/mL), bovine basic fibroblast growth factor (1 ng/mL, Roche, Switzerland), insulin (2.5 µg/mL), transferrin (2.5 µg/mL), sodium selenite (2.5 ng/mL) and gentamicin (50 µg/mL). hCMEC/D3 cells (passage number ≤ 35) were cultured for 3-5 days until full confluency and received 10 mM lithium chloride (Merck, USA) 24 hours before experiments to induce BBB properties [25, 12].

2.2.5. MTT Toxicity Assay

To test the viability and metabolic activity of brain endothelial cells after treatment with SNPs cellular reduction of the yellow 3-(4,5-dimethylthiazol-2-yl)-2,5-diphenyltetrazolium bromide (MTT) dye to formazan crystals was used [26]. Confluent cultures of brain endothelial cells in 96-well plates (Orange Scientific, Braine-l'Alleud, Belgium) were treated with SNPs diluted in culture medium in the concentration range of 0.01–1 mg/mL for 24 hours. Triton X-100 detergent (1 mg/mL) was used as a reference substance to determine the 100% cellular toxicity. After treatment

MTT solution (0.5 mg/ mL) was added to the wells for 3 hours at 37°C. Formazan produced by living cells was dissolved in dimethyl sulfoxide. Absorbance was detected by a multiwell plate reader at 570 nm (Fluostar Optima, BMG Labtechnologies, Ortenberg, Germany). Cell viability and metabolic activity are reflected by the MTT dye conversion and was calculated as the percentage of dye reduction by culture medium treated (control) cells.

2.2.6. Measurement of the Uptake of SNPs in Brain Endothelial Cells

Brain endothelial cell were seeded in 24-well plates (Corning Costar) at the density of 2×10^4 cells/well. After 3 days the confluent monolayers were incubated with 150 µg/mL SNP, SNP-B or SNP-B-GSH for 4 or 8 hours at 37 ºC in a CO_2 incubator. After incubation the cells were washed three times with ice cold PBS and lysed in 500 µL/well Triton X-100 detergent (10 mg/mL). To quantify the uptake of SNPs the fluorescence of cell lysates was measured with a spectrofluorometer (Horiba Jobin Yvon Fluorolog 3, Edison New Jersey, USA) at 488 nm excitation and 605 nm emission wavelengths.

To visualize the cellular uptake of the fluorescent particles brain endothelial cells were grown on collagen coated glass cover slips (VWR, USA) and treated with 150 µg/ml SNP, SNP-B or SNP-B-GSH for 24 hours. Cells were fixed with 4% paraformaldehyde in PBS for 30 min, washed three times with PBS then cell nuclei were stained with bis-benzimide (Hoechst dye 33342) for 10 min. Samples were mounted with Fluoromount-G (Southern Biotech, Birmingham, AL, USA), and examined with a confocal laser scanning microscope (Olympus Fluoview FV1000, Olympus Life Science Europa GmbH, Hamburg, Germany).

2.2.7. Permeability Measurement

For permeability studies brain endothelial cells were seeded onto collagen coated 12-well tissue culture inserts (Transwell clear, polyester membrane, 0.4 µm pore size, Corning Costar, USA) and cultured for 5 days. Culture medium was changed and resistance checked every second day. The integrity of the monolayers was checked by Evans blue labeled bovine serum albumin (Mw: 67 kDa) marker molecule. The cells were treated with 150 µg/mL SNP, SNP-B or SNP-B-GSH diluted in culture medium in the upper compartments (0.5 mL) for 8 hours. After incubation samples were collected from the lower compartments (1.5 mL) and measured with spectrofluorometer Horiba Jobin Yvon Fluorolog 3 at 488 nm excitation and 605 nm emission wavelengths for the SNPs and with Fluostar Optima at 584 nm excitation and 680 nm emission wavelengths for Evans blue-albumin. The apparent permeability coefficients (P_{app}, cm/s) were calculated as described previously [27] by the following equation:

$$P_{app}(\text{cm/s}) = \frac{\Delta[C]_A \times V_A}{A \times [C]_D \times \Delta t}$$

Briefly, P_{app} was calculated from the concentration difference of the nanoparticles in the lower or acceptor compartment ($\Delta[C]_A$) after 4 hours and $[C]_D$ is the concentration in the donor (upper) compartments at 0 hour, and V_A is the volume of the acceptor compartment (1.5 mL), and A is the surface area available for permeability (1.1 cm^2).

2.2.8. RNA Isolation and Quality Control

Rat brain microvessels were isolated as described in our previous article [28]. Primary brain endothelial cells (isolated and cultured according to the method described in our previous studies [28, 29]) and hCMEC/D3 cells were cultured for 5 days in 10 cm dishes. After reaching confluency cells were scraped and collected by centrifugation. Microvessel and cell pellets were used for total RNA isolation using RNAqueous-4PCR Kit (Ambion, Life Technologies, Austin, TX, USA) with DNase1 (RNase-free) treatment according to the manufacturer's instructions. The concentrations and purity of the DNase-treated RNA samples was assessed by a NanoDrop ND-1000 spectrophotometer (NanoDrop Technologies, Rockland, DE). The integrity of the isolated RNA was checked by Bioanalyzer 2100 (Agilent Technologies, Santa Clara, CA). The RNA integrity number (RIN) was 9.2-10 in the case of all studied RNA samples.

2.2.9. Quantitative Real-Time Polimerase Chain Reaction and Data Analysis

Quantitative real-time PCR (RT-PCR) and data analysis were performed as described in our previous study [30]. The cDNA synthesis was performed on 1 µg total RNA samples by High Capacity cDNA Reverse Transcription Kit (Life Technologies) using random hexanucleotides primers and MultiScribe Reverse Transcriptase in the presence of RNase inhibitor according to the manufacturer's standard protocols. The expression of the SMVT/SLC5A6 vitamin transporter gene was analyzed by quantitative PCR using TaqMan Low Density Array 384-well microfluidic cards preloaded with inventoried TaqMan Gene Expression Assays (for hCMEC/D3 human brain cells: Hs00221573_m1, for rat brain cells: Rn00590633_m1; Life Technologies). RT PCRs were performed by ABI TaqMan Universal Master Mix (Life Technologies) using the ABI Prism 7900 system (Applied Biosystems, Life Technologies). RT-PCR data were analyzed using the ABI SDS 2.0 software (Applied Biosystems, Life Technologies). In all samples the expression of genes was normalized to 18S rRNA, which was used as an endogenous control (ΔCt = Ctgene - Ct18S rRNA). Expression values reflecting the activity of studied genes were determined based on the normalized expression of genes calculated with 2-ΔCt formula which were correlated to the lowest normalized expression measured by the applied RT-PCR method. For quantification of relative expression level of genes of interest the normalized expression data were analyzed using the comparative ΔΔCt method.

2.2.10. Statistical Analysis

Data are presented as means ± SEM or SD. Values were compared using one-way or two-way analysis of variance following Dunnett or Bonferroni multiple comparison posttests (GraphPad-Prism 5.0; GraphPad Software, USA). Changes were considered statistically significant at $P < 0.05$. All experiments were repeated at least two times, the number of parallel samples was 4-8.

3. RESULTS

Table **1** summarizes the main physicochemical characteristics of the untargeted and targeted SNPs (for schematic drawing see Fig. **1**).

Table 1. Characterization of the non-targeted and targeted solid nanoparticles.

Nanoparticle	Size (nm)	Polydispersity index	Zeta potential (mV)
SNP	93 ± 0.59	0.131 ± 0.02	-14 ± 0.87
SNP-B	118.1 ± 2.9	0.251 ± 0.001	-23.1 ± 0.62
SNP-B-GSH	120.5 ± 2.86	0.261 ± 0.01	-23.8 ± 1.33

Values presented are means ± SD. SNP, non-targeted solid nanoparticles; SNP-B, biotin-targeted solid nanoparticles; SNP-B-GSH, glutathione-targeted solid nanoparticles.

The commercially available solid fluorescent particles (nominal size of 40 nm) were already functionalized with neutravidin which enlarged the SNPs. These neutravidin-coated particles were labeled with biotin and glutathione which further increased their size. All SNPs had low polydispersity index, indicating a relatively narrow size distribution. The average zeta potential for both targeted particles was very similar. The charge of the non-labeled SNP was less negative. The morphology of the nanoparticles was observed by

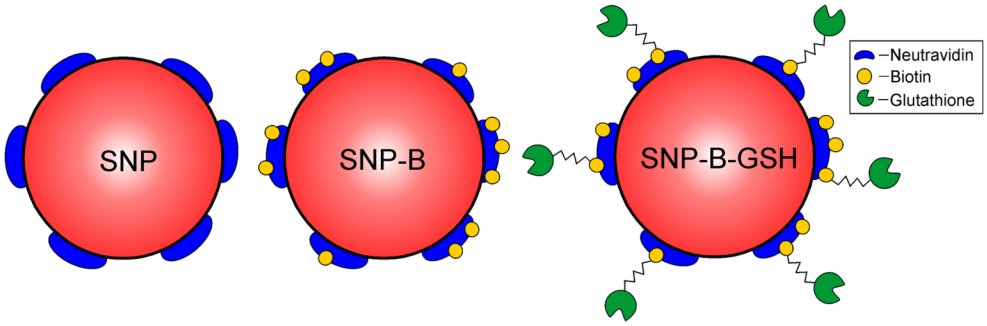

Fig. (1). Schematic drawing of non-targeted (SNP), biotin- (SNP-B) and glutathione-labeled (SNP-B-GSH) solid nanoparticles.

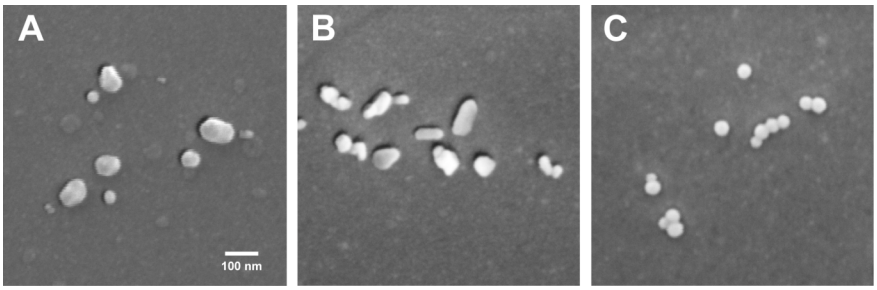

Fig. (2). Scanning electron microscopy images of non-targeted (A), biotin-targeted (B), and glutathione-targeted (C) solid nanoparticles. Bar: 100 nm.

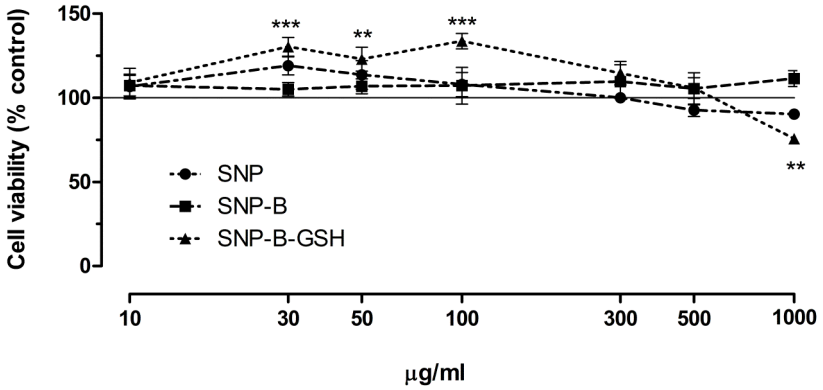

Fig. (3). The effect of non-targeted (SNP), biotin-targeted (SNP-B), and glutathione-targeted (SNP-B-GSH) solid nanoparticles on the viability of brain endothelial cells (24 hours). Values presented are means ± SEM. Statistical analysis: one-way analysis of variance followed by Dunnett's posttest, ** $P < 0.01$; *** $P < 0.001$ compared to control. n = 4-8. X-axis: log-10 scale.

SEM and shown on Fig. **2**. The particles had mostly spherical shapes, but some SNPs were elongated. The size of the SNPs were all in the same range, and corresponds well to data measured by dynamic light scattering. No aggregation was visible.

3.1. Effect of SNPs on the Cell Viability of Brain Endothelial Cells

Incubation of the brain endothelial monolayers with SNP and SNP-B in the 10-1000 µg/mL concentration range for 24 hours had no effect on cell viability assessed by MTT dye conversion (Fig. **3**). As a comparison, the reference substance Triton X-100 detergent decreased the cell viability below 10% of the control values. SNP-B-GSH (30-100 µg/mL) increased the metabolic activity of cells, while the highest concentration (1000 µg/mL) caused a reduction in viability (Fig. **3**). For further experiments we selected the 150 µg/mL concentration for all three SNPs, which can be considered as non-toxic.

3.2. Uptake of SNPs in Brain Endothelial Cells

The uptake of SNPs in endothelial cells was tested at two time points (Fig. **4**). In the design of our study we determined the time points for the uptake experiments based on the results of Gaillard *et al.* obtained on nanoparticles labeled with GSH, our reference ligand [31, 19, 20]. To be able to compare our data to these previous observations we selected 4 and 8 hours incubations. After 4 hours of incubation no significant difference between the uptakes of three SNPs in brain endothelial cells could be measured, although an increasing trend was seen in case of targeted SNPs. After 8-hour incubation the uptake of all tested nanoparticles was significantly higher compared to the 4-hour group. Importantly the uptake of the biotin- and glutathione-targeted SNPs was significantly increased; it was two times higher than the uptake of the non-targeted particle.

The uptake of the fluorescent nanoparticles could be visualized in brain endothelial cells by confocal microscopy (Fig. **5**). Red

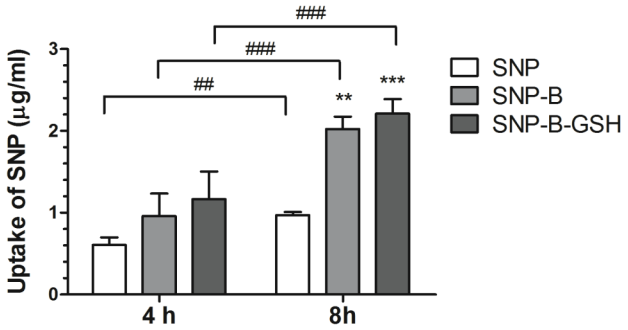

Fig. (4). The uptake of non-targeted (SNP), biotin-labeled (SNP-B) and glutathione-labeled (SNP-B-GSH) solid nanoparticles in brain endothelial cells after 4 or 8 hours incubation. The concentration of SNPs is 150 µg/mL in each group. Values presented are means ± SEM. Statistical analysis: two-way analysis of variance followed by Bonferroni posttest, where $^{**}P < 0.01$; $^{***}P < 0.001$, compared to SNP treated group, $^{\#\#}P < 0.01$; $^{\#\#\#}P < 0.001$, compared to the 4 hour-incubation group; n = 4–6.

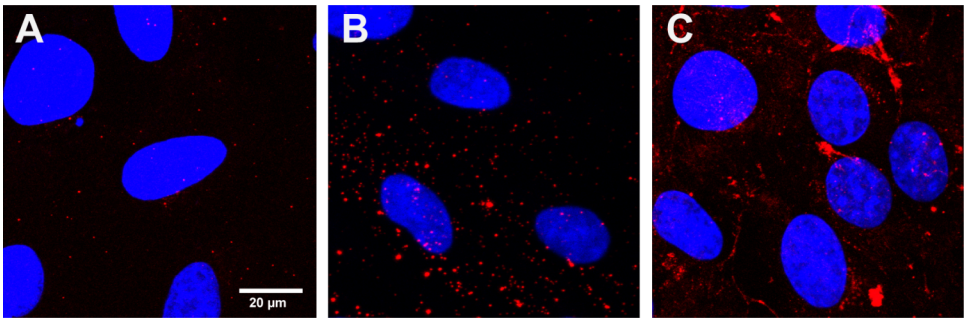

Fig. (5). Confocal microscopy images of cultured human brain endothelial cells incubated with non-labeled (A), biotin-labeled (B), and glutathione-labeled (C) solid nanoparticles (red) for 8 hours at 37 ºC. The concentration of SNPs is 150 µg/mL in each group. Cell nuclei were stained with bis-benzimide (blue). Bar: 20 µm.

fluorescent dots can be seen in the cytoplasm of the cells treated with SNPs. More fluorescent particles were seen in cells incubated with glutathione-labeled SNPs indicating better uptake of these nanoparticles as compared to the non-targeted SNPs.

3.3. Penetration of SNPs Across Brain Endothelial Monolayers

The permeability of hCMEC/D3 brain endothelial cell monolayers for Evans blue-albumin was 1.6 ± 0.3 $\times 10^{-6}$ cm/s which was in the same range as in our previous study [32] and reflects a suitable barrier for testing SNPs. All SNPs crossed the brain endothelial layers in the permeability tests but at different extent (Fig. **6**). After 8-hour incubation the P_{app} of biotin targeted SNP was 2.8 fold higher than that of the non-targeted SNP. The penetration of the GSH targeted nanoparticles was the highest, a significant, 5.8 fold increase was measured as compared to the unlabeled SNP group.

3.4. Expression of SMVT/SLC5A6 mRNA in Brain Microvessels and Cultured Brain Endothelial Cells

The expression level of SMVT/SLC5A6 vitamin transporter gene mRNA was expressed in isolated rat brain microvessels, and both in hCMEC/D3 human brain endothelial cell line and primary rat brain endothelial cells (Fig. **7**). No statistically significant change was found in the mRNA expression level between the groups (one-way ANOVA and Bonferroni posttest).

4. DISCUSSION

Although drug delivery systems to cross the BBB are an intensely researched area there are no targeted nanoparticles in the human therapy yet to deliver therapeutics to the brain in a controlled and non-invasive manner. Specific targeting can be achieved

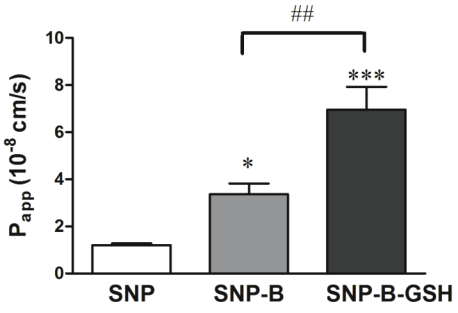

Fig. (6). Permeability changes of brain endothelial monolayers after SNP treatments (150 µg/mL, 8 h). Values presented are means ± SEM. Statistical analysis: one-way analysis of variance followed by Bonferroni posttest. $^{*}P < 0.05$, $^{***}P < 0.001$, compared to non-labeled SNP treated group; $^{\#\#}P < 0.01$, compared to biotin-labeled SNP treated group, n = 6.

through exploiting the physiological transport pathways of the BBB including the endogenous nutrient transporters of brain endothelium [2, 7]. Despite the abundance of carrier mediated transporters at the BBB this physiological pathway is still not fully exploited for drug delivery.

Biotin is a potential BBB targeting ligand, since it has a highly expressed carrier, SLC5A6, at the human BBB including hCMEC/D3 brain endothelial cells [23, 30]. We have verified the presence of SLC5A6 mRNA in hCMEC/D3 brain endothelial cells, which showed an expression level similar to isolated brain

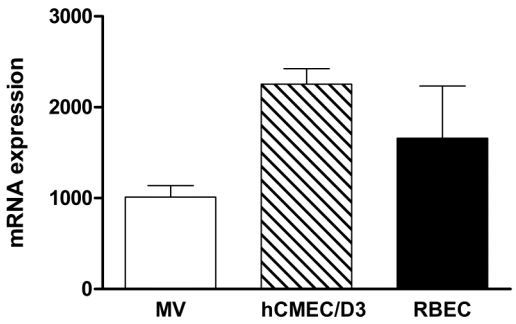

Fig. (7). The expression level of SMVT/SLC5A6 vitamin transporter gene mRNA in isolated rat brain microvessels (MV), hCMEC/D3 human brain endothelial cell line and primary rat brain endothelial cells (RBEC).

microvessels and cultured primary brain endothelial cells. Biotin is a cofactor for several carboxylase enzymes and a cell growth promoter. It cannot be synthesized endogenously in the brain therefore it is supplied from the blood across the BBB. The brain concentration of biotin is about 50-fold higher than that in the plasma [33].

Biotin technology based on the exceptionally strong binding between biotin and avidin has long been used in basic research for immunohistochemistry and molecular biology. Recently biotin-avidin technology has been applied for drug targeting to tumors [24]. In several studies nanoparticles are biotinylated to easily detect them on tissue slices with streptavidin-FITC [34]. Biotinylation of drugs is also used to bind them to avidin-functionalized particles [35]. However, none of the studies used biotin as a ligand for BBB targeting.

We prepared and characterized biotin- and glutathione-labeled SNPs from neutravidin-coated commercially available red fluorescent polystyrene particles. Labeling with biotin and biotin-glutathione increased the particle size, in accordance with literature data on biotinylated albumin NPs [34]. The average size and surface charge of the targeted SNPs were similar measured by dynamic light scattering. The heterogeneity seen by scanning electron microscopy may be related to the different batches of SNPs used for labeling. The size of NPs related to their cellular uptake and biodistribution is widely studied. In general, particles with a size below 100 nm can be taken up by all cells by endocytosis and are considered as high risk NPs from nanotoxicology point of view, especially if they are non-biodegradable [36]. These small NPs are non-specifically taken up by the liver, lungs and kidneys. This is the reason why most NPs developed for possible therapeutic use has a size in the range of 100-200 nm. The glutathione targeted NPs used by Gaillard and his colleagues were also in this range, e.g. 108 nm, [31]; 95 nm, [20]. The size of SNPs used in this study fell also in this range. NPs larger, than 200 nm do not enter brain tissue [37]. In agreement with *in vivo* findings NPs with 400 nm size did not cross a culture BBB model [38].

We are the first to demonstrate, that biotin-labeling increases the uptake and transfer of SNPs in human brain endothelial cells as compared to unlabeled particles. This finding is in agreement with active transport of biotin at the BBB *in vivo* [39] and in hCMEC/D3 brain endothelial cell cultures [23]. An experimental study indicates that biotinylated NPs can enter the brain [34] and this targeting concept may work *in vivo*, too. Intravenously administered biotinylated albumin NPs could be detected in several brain regions of rats with experimental autoimmune encephalomyelitis using *post mortem* streptavidin-FITC labeling [34]. However, this observation may provide indirect support only, because the aim of this study was the visualization of albumin NPs in the CNS, and no data are available in control rats or with unlabeled albumin NPs.

We showed a high uptake for the biotinylated glutathione-labeled SNPs in brain endothelial cells. Gaillard *et al*. proved in several studies the increased uptake of glutathione-labeled pegylated liposomes in both cultured rat and human endothelial cells [31, 20]. We found that the transfer of glutathione-labeled SNPs across the *in vitro* BBB model was the highest among the tested particles and several fold higher than that of the non-targeted ones. Our results are in concordance with the *in vivo* data on the enhanced brain penetration of drugs and biopharmacons, including cytostatic doxorubicin, antiinflammatory methylprednisolone, opioid peptide DAMGO, and an anti-amyloid antibody by glutathione-labeled vesicular NPs. Glutathione as a vector not only increased the brain delivery of doxorubicin (543 Da) in rats [21], but it also inhibited tumor growth and increased survival in a mouse model of glioblastoma multiforme [20]. Brain uptake of methylprednisolone (374 Da) was elevated by glutathione targeting [19], and improved therapeutic efficacy was described for GSH-pegylated liposomal methylprednisolone in experimental autoimmune encephalomyelitis in rats [19], in mice [40], and in ocular inflammation in rats [41]. Increased brain delivery was demonstrated for the opioid pentapeptide DAMGO (513 Da) by GSH-pegylated liposomes in rats [22]. Enhanced GSH-pegylated liposomal brain delivery of a llama single domain anti-amyloid antibody fragment (15 kDa) was demonstrated in a mouse model for Alzheimer's disease [42], indicating that the platform may also be used for CNS delivery of biopharmacons.

Targeted NPs may use several transport routes at the BBB as reviewed by Rempe *et al*. [43]. Solid NPs were described to cross brain endothelial cells by receptor- or adsorption-mediated transcytosis [36, 43]. The higher transfer of SNP-B and SNP-B-GSH particles may be related to transcytosis due to the binding of targeting ligands to the surface of the brain endothelial cells. Indeed, we have verified the presence of SMVT/SLC5A6 mRNA in hCMEC/D3 brain endothelial cells, our BBB model system. In the case of biotin targeted SNPs, we hypothesize that the targeting ligand helps the binding of the nanocarriers to the surface of brain endothelial cells, which triggers transcytosis across the brain endothelial monolayers. For the clinical-stage GSH drug delivery platform, although the BBB receptor/transporter is unknown, the suggested mechanism of BBB crossing is a secific liposomal endocytosis pathway indicative of receptor-mediated transcytosis [19]. Further experiments are needed to explore the exact mechanism.

CONCLUSION

Biotin as a ligand increased the uptake and the transfer of nanoparticles across brain endothelial cells and may have a potential to be used as a BBB targeting molecule. Biotinylated glutathione was more effective as a ligand to increase nanoparticle permeability through endothelial monolayers supporting its use as successful brain targeting vector.

LIST OF ABBREVIATIONS

ACN	=	Acetonitrile
B	=	Biotin
BBB	=	Blood-brain barrier
DCC	=	*N,N*-dicyclohexyl-carbodiimide
DCM	=	Dichloromethane
DIEA	=	*N,N*-diisopropylethylamine
DMF	=	*N.N*-dimethylformamide
DTT	=	1,4-dithiothreitol
Fmoc	=	9-flourenylmethyloxycarbonyl
GSH	=	Glutathione

HATU	=	1-[Bis(dimethylamino)methylene]-1H-1,2,3-triazolo[4,5-b]pyridinium 3-oxid hexafluorophosphate
hCMEC/D3	=	Human brain endothelial cell line
HOBt	=	1-hydroxybenzotriazole
HPLC	=	High performance liquid chromathography
MTT	=	3-(4,5-dimethylthiazol-2-yl)-2,5-diphenyltetrazolium bromide
NP	=	Nanoparticle
SLC	=	Solute carrier transporter
SNP	=	Solid nanoparticle
SNP-B	=	Biotin targeted solid nanoparticle
SNP-B-GSH	=	Biotinylated-glutathione targeted solid nanoparticle
TFA	=	Triflouroacetic acid
TIS	=	Triisopropylsilane

CONFLICT OF INTEREST

The authors declare that there is no conflict of interest in connection to the present work.

ACKNOWLEDGEMENTS

This work was supported by the Hungarian Scientific Research Fund (OTKA PD105622) and by the National Research, Development and Innovation Office (GINOP-2.2.1-15-2016-00007, GINOP-2.3.2-15-2016-00060). S.V. was supported by the János Bolyai Research Fellowship of the Hungarian Academy of Sciences (BO/00724/12).

REFERENCES

[1] Neuwelt EA, Bauer B, Fahlke C, *et al.* Engaging neuroscience to advance translational research in brain barrier biology. Nat Rev Neurosci 2011; 12(3): 169-82.

[2] Pardridge WM. Drug transport across the blood-brain barrier. J Cereb Blood Flow Metab 2012; 32(11): 1959-72.

[3] Abbott NJ, Patabendige AA, Dolman DE, *et al*. Structure and function of the blood-brain barrier. Neurobiol Dis 2010; 37(1): 13-25.

[4] Deli MA. Drug transport and the blood-brain barrier. In: Tihanyi K, Vastag M, editors. Solubility, Delivery, and ADME Problems of Drugs and Drug-Candidates. Washington: Bentham Science Publishers Ltd.; 2011. p. 144-65.

[5] Kreuter J. Drug delivery to the central nervous system by polymeric nanoparticles: what do we know? Adv Drug Deliv Rev 2014; 71: 2-14.

[6] Veszelka S, Bocsik A, Walter F, *et al*. Blood-brain-barrier coculture models to study nanoparticle penetration: focus on coculture systems. Acta Biol Szeged 2015; 59(Suppl.2): 157-68.

[7] Pardridge WM. Blood-brain barrier endogenous transporters as therapeutic targets: a new model for small molecule CNS drug discovery. Expert Opin Ther Targets 2015; 19(8): 1059-72.

[8] Campos-Bedolla P, Walter FR, Veszelka S, *et al.* Role of the blood-brain barrier in the nutrition of the central nervous system. Arch Med Res 2014; 45(8): 610-38.

[9] Enerson BE and Drewes LR. The rat blood-brain barrier transcriptome. J Cereb Blood Flow Metab 2006; 26(7): 959-73.

[10] César-Razquin A, Snijder B, Frappier-Brinton T, *et al.* A call for systematic research on solute carriers. Cell 2015; 162(3): 478-87.

[11] Gromnicova R, Davies HA, Sreekanthreddy P, *et al.* Glucose-coated gold nanoparticles transfer across human brain endothelium and enter astrocytes *in vitro*. PLoS One 2013; 8(12): e81043.

[12] Weksler B, Romero IA, Couraud PO. The hCMEC/D3 cell line as a model of the human blood brain barrier. Fluids Barriers CNS 2013; 10(1): 16.

[13] Helms HC, Abbott NJ, Burek M, *et al. In vitro* models of the blood-brain barrier: An overview of commonly used brain endothelial cell culture models and guidelines for their use. J Cereb Blood Flow Metab 2016; 36(5): 862-90.

[14] Dufes C, Gaillard F, Uchegbu IF, *et al.* Glucose-targeted niosomes deliver vasoactive intestinal peptide (VIP) to the brain. Int J Pharm 2004; 285(1-2): 77-85.

[15] Vyas A, Jain A, Hurkat P, *et al.* Targeting of AIDS related encephalopathy using phenylalanine anchored lipidic nanocarrier. Colloids Surf B Biointerfaces 2015; 131: 155-61.

[16] Li J, Guo Y, Kuang Y, *et al.* Choline transporter-targeting and co-delivery system for glioma therapy. Biomaterials 2013; 34(36): 9142-8.

[17] Kannan R, Chakrabarti R, Tang D, *et al.* GSH transport in human cerebrovascular endothelial cells and human astrocytes: evidence for luminal localization of Na+-dependent GSH transport in HCEC. Brain Res 2000; 852(2): 374-82.

[18] Gaillard PJ. BBB crossing assessment and BBB crossing technologies in CNS Drug Discovery. Drug Discov Today Technol 2016; 20: 1-3.

[19] Gaillard PJ, Appeldoorn CC, Rip J, *et al*. Enhanced brain delivery of liposomal methylprednisolone improved therapeutic efficacy in a model of neuroinflammation. J Control Release 2012; 164: 364-9.

[20] Gaillard PJ, Appeldoorn CC, Dorland R, *et al*. Pharmacokinetics, brain delivery, and efficacy in brain tumor-bearing mice of glutathione pegylated liposomal doxorubicin (2B3-101). PLoS One 2014; 9(1): e82331.

[21] Birngruber T, Raml R, Gladdines W, *et al.* Enhanced doxorubicin delivery to the brain administered through glutathione PEGylated liposomal doxorubicin (2B3-101) as compared with generic Caelyx,(®)/Doxil(®)--a cerebral open flow microperfusion pilot study. J Pharm Sci 2014; 103(7): 1945-8.

[22] Lindqvist A, Rip J, van Kregten J, *et al.* Hammarlund-Udenaes M. *In vivo* functional evaluation of increased brain delivery of the opioid peptide DAMGO by glutathione-PEGylated liposomes. Pharm Res 2016; 33(1): 177-85.

[23] Uchida Y, Ito K, Ohtsuki S, *et al*. Major involvement of Na^+-dependent multivitamin transporter (SLC5A6/SMVT) in uptake of biotin and pantothenic acid by human brain capillary endothelial cells. J Neurochem 2015; 134(1): 97-112.

[24] Lesch HP, Kaikkonen MU, Pikkarainen JT, *et al*. Avidin-biotin technology in targeted therapy. Expert Opin Drug Deliv 2010; 7(5): 551-64.

[25] Liebner S, Corada M, Bangsow T, *et al.* Wnt/beta-catenin signaling controls development of the blood-brain barrier. J Cell Biol 2008; 183(3): 409-17.

[26] Kiss L, Walter FR, Bocsik A, *et al*. Kinetic analysis of the toxicity of pharmaceutical excipients Cremophor EL and RH40 on endothelial and epithelial cells. J Pharm Sci 2013; 102(4): 1173-81.

[27] Bocsik A, Darula Z, Tóth G, *et al.* Transfer of opiorphin through a blood-brain barrier culture model. Arch Med Res 2015; 46(6): 502-6.

[28] Veszelka S, Pásztói M, Farkas AE, *et al.* Pentosan polysulfate protects brain endothelial cells against bacterial lipopolysaccharide-induced damages. Neurochem Int 2007; 50(1): 219-28.

[29] Nakagawa S, Deli MA, Kawaguchi H, *et al.* A new blood-brain barrier model using primary rat brain endothelial cells, pericytes and astrocytes. Neurochem Int 2009; 54(3-4): 253-63.

[30] Tóth AE, Tóth A, Walter FR, *et al.* Compounds blocking methylglyoxal-induced protein modification and brain endothelial injury. Arch Med Res 2014; 45(8): 753-64.

[31] Rip J, Chen L, Hartman R, *et al*. Glutathione PEGylated liposomes: pharmacokinetics and delivery of cargo across the blood-brain barrier in rats. J Drug Target 2014; 22(5): 460-7.

[32] Walter FR, Valkai S, Kincses A, *et al*. A versatile lab-on-a-chip tool for modeling biological barriers. Sens Actuators B Chem 2016; 222: 1209-19

[33] Spector R, Johanson CE. Vitamin transport and homeostasis in mammalian brain: focus on Vitamins B and E. J Neurochem 2007; 103(2): 425-38.

[34] Merodio M, Irache JM, Eclancher F, *et al.* Distribution of albumin nanoparticles in animals induced with the experimental allergic encephalomyelitis. J Drug Target 2000; 8(5): 289-303.

[35] Neves AR, Queiroz JF, Weksler B, *et al.* Solid lipid nanoparticles as a vehicle for brain-targeted drug delivery: two new strategies of functionalization with apolipoprotein E. Nanotechnology 2015; 26(49): 495103

[36] Müller RH, Gohla S, Keck CM. State of the art of nanocrystals—special features, production, nanotoxicology aspects and intracellular delivery. Eur J Pharm Biopharm 2011; 78(1): 1-9.

[37] Mc Carthy DJ, Malhotra M, O'Mahony AM, *et al.* Nanoparticles and the blood-brain barrier: advancing from in-vitro models towards therapeutic significance. Pharm Res 2015; 32(4): 1161-85.

[38] Hanada S, Fujioka K, Inoue Y, *et al.* Cell-based *in vitro* blood-brain barrier model can rapidly evaluate nanoparticles' brain permeability in association with particle size and surface modification. Int J Mol Sci 2014; 15(2): 1812-25.

[39] Spector R, Mock D. Biotin transport through the blood-brain barrier. J Neurochem 1987; 48(2): 400-4.

[40] Lee DH, Rötger C, Appeldoorn CC, *et al.* Glutathione PEGylated liposomal methylprednisolone (2B3-201) attenuates CNS inflammation and degeneration in murine myelin oligodendrocyte glycoprotein induced experimental autoimmune encephalomyelitis. J Neuroimmunol 2014; 274(1-2): 96-101.

[41] Reijerkerk A, Appeldoorn CC, Rip J, *et al.* Systemic treatment with glutathione PEGylated liposomal methylprednisolone (2B3-201) improves therapeutic efficacy in a model of ocular inflammation. Invest Ophthalmol Vis Sci 2014; 55(4): 2788-94.

[42] Rotman M, Welling MM, Bunschoten A, *et al*. Enhanced glutathione PEGylated liposomal brain delivery of an anti-amyloid single domain antibody fragment in a mouse model for Alzheimer's disease. J Control Release 2015; 203: 40-50.

[43] Rempe R, Cramer S, Qiao R, *et al.* Strategies to overcome the barrier: use of nanoparticles as carriers and modulators of barrier properties. Cell Tissue Res 2014; 355(3): 717-26.